ELSEVIER

4 April 1997

Chemical Physics Letters 268 (1997) 101–106

CHEMICAL PHYSICS LETTERS

Helicity and packing of single-walled carbon nanotubes studied by electron nanodiffraction

Lu-Chang Qin [a], Sumio Iijima [a], Hiromichi Kataura [b], Yutaka Maniwa [b], Shinzo Suzuki [c], Yohji Achiba [c]

[a] *NEC Corporation, Fundamental Research Laboratories, 34 Miyukigaoka, Tsukuba, Ibaraki 305, Japan*
[b] *Tokyo Metropolitan University, Department of Physics, Hachioji, Tokyo 192-03, Japan*
[c] *Tokyo Metropolitan University, Department of Chemistry, Hachioji, Tokyo 192-03, Japan*

Received 8 November 1996

Abstract

Electron nanodiffraction patterns from raft-like bundles of single-walled carbon nanotubes have been obtained to analyze the helicity distribution and the packing of the tubules. In most cases, the helical angles were found to be quite evenly distributed, ranging from the zigzag structure of 0° helicity to the armchair structure of 30° helicity. Examples of preferred helicities were encountered occasionally, such as bundles of tubules of almost single-helicity, corresponding to the armchair structure. The lattice constant of the hexagonally packed bundles varied and two example values were determined to be 1.64 nm and 1.71 nm, respectively.

1. Introduction

One of the unique features of the seamless carbon nanotubes discovered by Iijima [1] is that they often have helical structures, as indicated by their electron diffraction patterns. This feature is common to both the multiwalled [1] and single-walled carbon nanotubes [2]. As has been predicted by theoretical studies, the helicities of carbon nanotubes have a profound effect on the physical properties of the tubules, such as electrical conductivity. Together with its diameter, for instance, a single-walled carbon nanotube can behave either as a metallic conductor or a semiconductor, depending on these parameters [3]. These characteristics therefore make it of vital importance to obtain the helicity of carbon nanotubes. However, due to the nanoscale dimensions of this new form of carbon, X-ray diffraction has not been very useful for determining the helicities of carbon nanotubes [4,5]. On the other hand, since electrons now can be focused to nanosized probes and they interact with matter much more strongly than X-rays do, electron nanodiffraction is so far the only practical technique to reveal the helicities of carbon nanotubes, and the strategy and an improved method have been established recently [6,7].

Recent advances in synthesis techniques [8,9] have now made possible the production of single-walled carbon nanotubes in large quantities at high yield. Crystalline bundles of carbon nanotubes in hexagonal close packing have been reported in the thus produced structures from electron microscopy and X-ray diffraction studies [4,5,9]. The lattice constant of such bundles has been reported to be about 1.70 nm from X-ray diffraction measurements [5] and

PII S0009-2614(97)00166-8

about 1.59 nm from cross-view high-resolution electron micrographs [9]. Though it has been suggested [5], based on theoretical argument, that the tubules that form the crystalline bundles are of single helicity, concrete experimental evidence has so far not been produced to substantiate this hypothesis. Given the uniqueness of this structure, it is certainly of great interest to examine the helicity distribution of the constituting tubules in such bundles.

In this Letter, theoretical background for elucidating helicities of single-walled carbon nanotubes is summarized and relevant equations are presented. Experimental results, obtained by using electron nanodiffraction technique, are given on the helicity distribution of selected raft-like bundles of single-walled carbon nanotubes which were produced by laser ablation of graphite powders catalyzed by a mixture of Ni and/or Co particles. When the bundles were aligned perpendicular to the incident electron beam, electron diffraction patterns from such bundles were also used to determine the lattice constant of the hexagonally packed structure. Two different bundles of single-walled carbon nanotubes were found to have lattice constants of 1.64 nm and 1.71 nm, respectively.

2. Theory

The electron scattering amplitude from an object can always be given by the generic expression for the total scattering amplitude

$$F(q) = \Sigma_j f_j(q)\exp\left[2\pi i q \cdot r_j\right], \qquad (1)$$

where f_j is the atomic scattering amplitude for electrons from the atom positioned at r_j, F the structure factor, and q the scattering vector defined by $q = 2\sin(\Theta/2)/\lambda$, in which Θ is the total scattering angle and λ the electron wavelength. In the polar coordinate framework, for a single-walled carbon nanotube of radius r, the above equation can be conveniently expressed in terms of the polar coordinates (R, Φ, l) in reciprocal space by the following equation [6]:

$$F(R,\Phi,l) = \Sigma_n \exp\left[in(\Phi + \pi/2)\right] J_n(2\pi r_0 R) \times \Sigma_j f_j \exp\left[i(n\phi_j + 2\pi l z_j/c)\right], \qquad (2)$$

where (ϕ_j, z_j) are polar coordinates of atom j, and J_n is the Bessel function of order n. Numerical calculations can be more conveniently carried out when the above equation is rewritten as

$$F_r(R,\Phi,l) = \Sigma_n B_n(R,\Phi) T_{nl}, \qquad (3)$$

where

$$T_{nl} = \Sigma_j f_j \exp\left[2\pi i(nx_j/a + lz_j/c)\right] \qquad (4)$$

describes the structure factor in radial projection and

$$B_n(R,\Phi) = \exp\left[in(\Phi + \pi/2)\right] J_n(2\pi rR) \qquad (5)$$

takes into account the scattering effect due to the cylindrical curvature of the nanotube. In Eq. (4), a is the length of the azimuthal edge $2\pi rR$ and c is the length of the axial edge, and therefore T_{nl} gives the structure factor of a two-dimensional array of the radial projection of the tubule cell (asymmetric unit). The term $B_n(R, \Phi)$ results from the cylindrical curvature of the tubule.

For a bundle of single-walled nanotubes of same diameter, the total scattering amplitude is the coherent sum of all the constituting individual tubules:

$$F_T \approx \Sigma_m F_m(R,\Phi,l)\exp(2\pi i \delta_m), \qquad (6)$$

where δ_m is the phase shift factor caused by relative rotations and translations of tubule m with respect to a chosen origin. These two parameters should make it incoherent the scattering characteristic of each individual tubule. Therefore, when this phase shift is random, the summation becomes incoherent, and the total intensity reduces to the sum of intensities. In other words, when the constituting tubules of a bundle scatter inherently, the total intensity distribution would be the sum of intensity from each tubule. Therefore, if the helicity distribution is uniform between the two extreme non-helical cases as given in calculations discussed later, a continuous intensity arc will be expected instead of spotty reflections. On the other hand, these two degrees of freedom do not change the packing of the tubules when they form raft-like bundles, where well defined positional correlation exists. This positional correlation, regardless of the relative translational and rotational disorder mentioned above, will give rise to sharp intensity peaks on the central row (perpendicular to the tubule axis) in the diffraction patterns. As a result, when

looking perpendicular to the tubule axis, the regular packing of tubules would also give rise to sharp reflections representing the positional correlation in the regular packing pattern. As has been revealed by cross-view electron micrographs, the packing assumes hexagonal geometry. Therefore the lattice

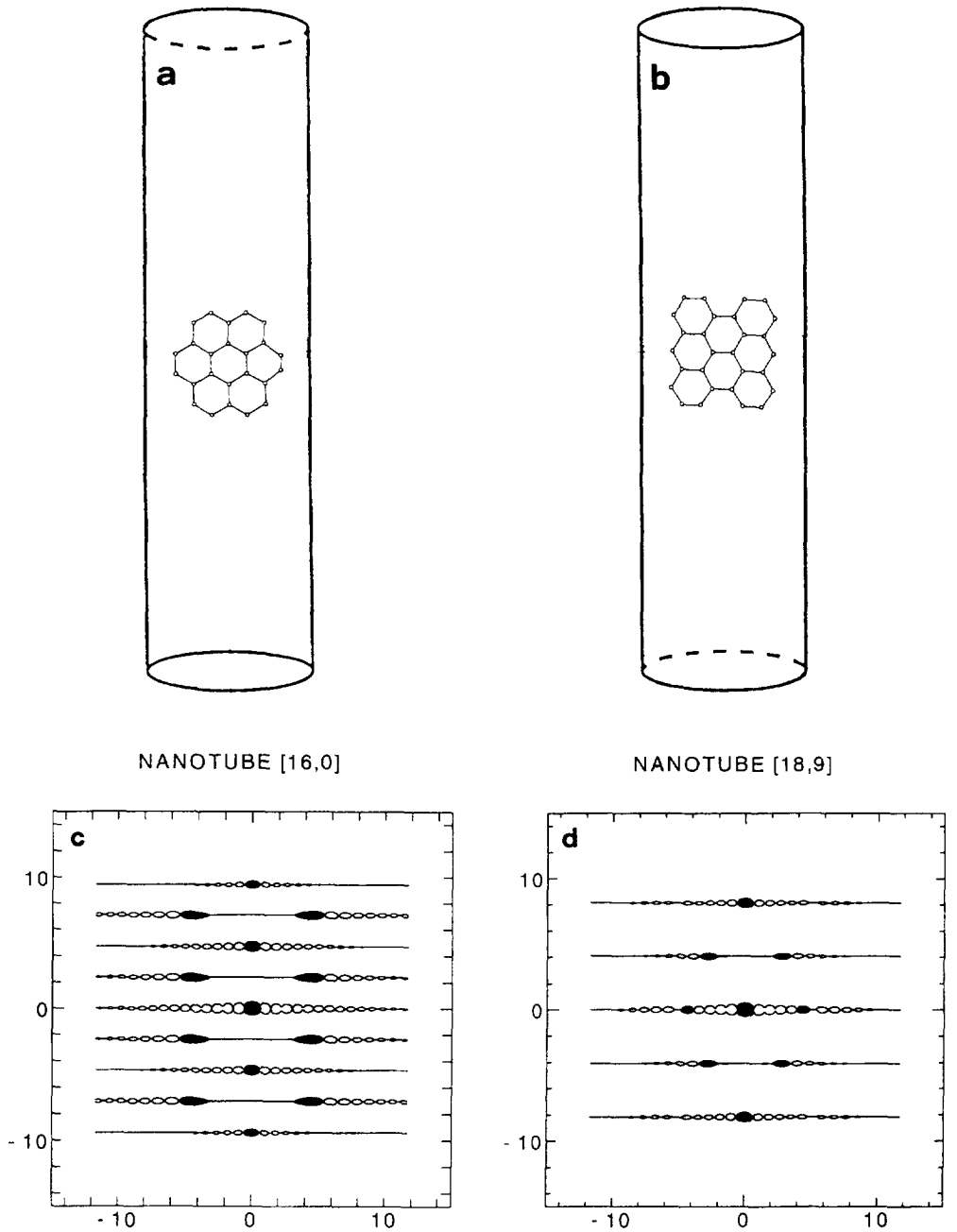

Fig. 1. Schematic drawings illustrating (a) the zigzag structure and (b) the armchair structure, whose helical angles are 0° and 30°, respectively. Corresponding calculated electron diffraction patterns are given in (c) and (d), corresponding to the zigzag structure and the armchair structure, respectively. The scaling unit for both axes is nm^{-1}.

constant of the super-lattice can easily be deduced when electron diffraction patterns from the tubule bundles when they are aligned at low index orientations, such as [100] or [120].

The helicity of a tubule is defined following the crystallographic convention as used in Ref. [6], where the angle between the two basis vectors is 120°. Other choice of the basis vectors, for example, the solid state physics convention where the angle between the two basis vectors is chosen to be 60°, will result in different indices for a given structure, though the final results will be equivalent to the former. Once the basis vectors are defined, two crystallographic indices that specify the perimeter of a cylindrical tubule will define the atomic structure of the tubule unambiguously if the handedness is neglected. The helical angles therefore fall between the two non-helical cases, i.e., the zigzag structure with indices $[u, 0]$ of helical angle 0° and the armchair structure with indices $[u, u/2]$ of helical angle 30°, as illustrated in Fig. 1a and b.

3. Results and discussion

Fig. 1a and b show the structural configurations of the two non-helical structures, i.e., the zigzag structure (Fig. 1a) and the armchair structure (Fig. 1b). The calculated corresponding electron diffraction intensities from these two structures are given in Fig. 1c and d, whose indices are [16, 0] (zigzag) and [18, 9] (armchair). Their diameters are 1.25 nm (zigzag) and 1.22 nm (armchair), respectively. In general, the scattering intensities from such carbon nanotubes can be divided into two classes: (a) the fundamental reflections from the graphene lattice that are well represented by enhanced intensities at the corresponding Bragg positions, which can be conveniently indexed using the hexagonal lattice indices, though these reflections are broadened; and (b) additional diffuse scattering intensities representing the shape function of the finite scattering tubules. Since the nanotube structure is still periodic along the tubule axis, intensities show up only on well defined layer lines. However, along each layer line, the scattering intensities were contributed by both the graphene reflection and the shape function. Fig. 1c and d are electron intensity distributions calculated using the equation given above for the two single-shelled carbon nanotubes schematically shown in Fig. 1a and b. On each layer line, the respective intensity increases with the height of the intensity blob above the layer line.

Fig. 2 shows an experimental electron nanodiffraction pattern from a thin bundle of about 50 single nanotubes, where the reflection intensities can be seen to have concentrated on arcs corresponding to (100) and (110) reflections, which were indicated by arrows in the figure. By comparing with the two calculated intensity maps shown in Fig. 1c and d, this continuous intensity distribution indicates that there was a quite uniform distribution of helicities between the two extreme cases, i.e., the 0° helicity of zigzag structure and the 30° helicity of the armchair structure.

Although most often we observed diffraction patterns showing continuous intensity arcs, as displayed in Fig. 2, Fig. 3 gives an electron nanodiffraction pattern from a different nanotube bundle. Here the reflection intensities were concentrated narrowly at the positions corresponding to the armchair configuration, whose diffraction geometry is given in Fig. 1d. This demonstrated that the bundle contained mostly tubules of armchair structure. In this pattern, the much diffused intensity distribution were resulted from the focused probe, which was utilized to avoid interference from neighboring structures. However, it should be noted here that this type of diffraction

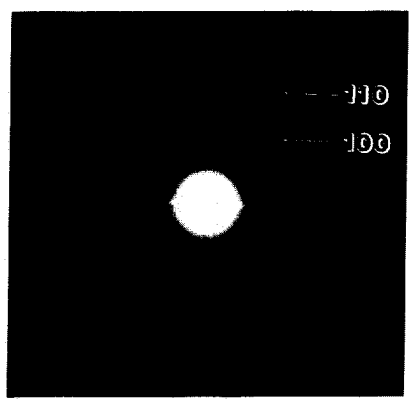

Fig. 2. Electron diffraction from a bundle of about 50 single tubules. The continuous intensity arcs indicate a uniform distribution of helicities among the constituting single nanotubes. The intensity arcs were indexed using the graphene lattice.

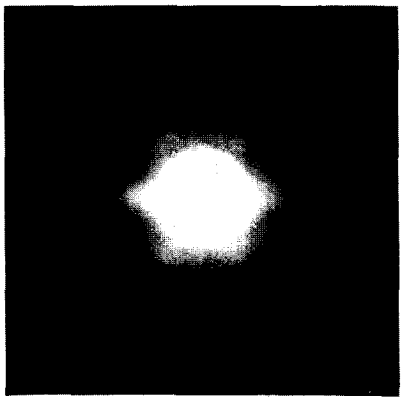

Fig. 3. Convergent-beam electron diffraction from a rarely encountered bundle of single-walled carbon nanotubes of almost single helicity corresponding the armchair structure shown schematically in Fig. 1 (d).

geometry, corresponding to bundles composed of tubules of single helicity, was not often observed in the materials we prepared.

As mentioned earlier, when the nanotubes form a bundle, depending on the positional correlation between the tubules, various coherence should occur when they scatter incident electron beams as an integral scattering object. Given two tubules in close-packing, there are still two degrees of freedom: (a) translation along the tubule axis and (b) relative rotation about the tubule axis, just like the case in fullerite at elevated temperature where rotational disorder occurs. Both factors will have effect on the coherence of electron diffraction. However, the low signal/noise ratio has made it practically impossible to obtain absolute scattering intensities, from which the coherence could be evaluated in principle.

Nonetheless, the packing of the tubules in a bundle can be revealed by both real-space electron micrographs and electron diffraction. Fig. 4 shows two electron nanodiffraction patterns from thick bundles which were able to give rise to high super reflection intensities representing the packing. Some of the super-structure reflections of high intensity are indicated by arrows in the figure. It is worth noting that the super reflections appeared only on the central row in the diffraction patterns. When the scattering bundle itself has no structural periodicity along the tubule axis, the super reflections appear only along the central row perpendicular to the axis. This is also indicative of the fact that the constituting tubules do not have a single helicity, because if it were the case, the bundle would have the same periodicity along

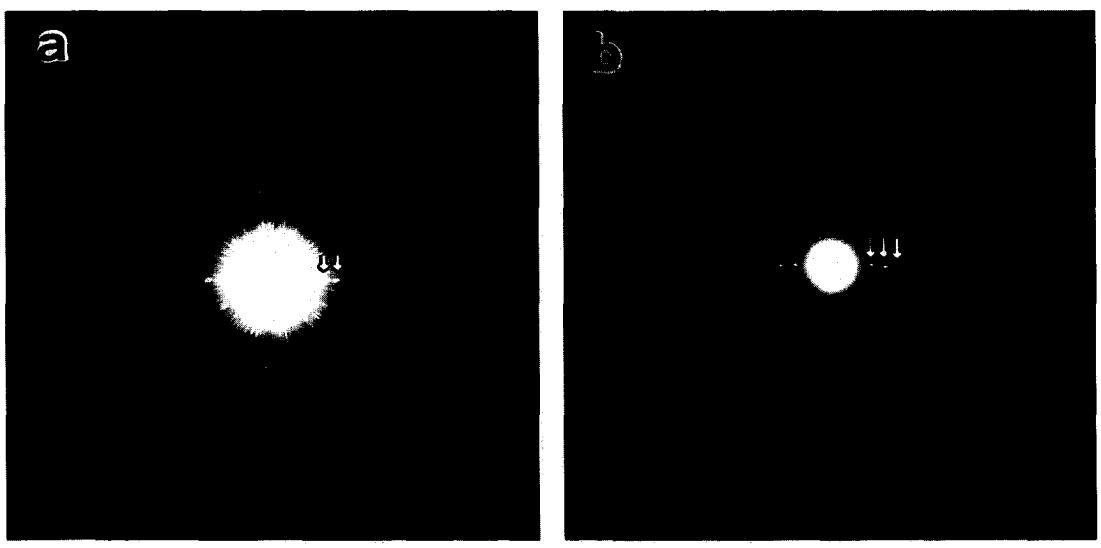

Fig. 4. Electron nanodiffraction patterns from thick bundles that give rise to super-structure reflections on the central row (indicated by arrows) representing positional correlation in the packing of the tubules. (a) Corresponding to hexagonal lattice constant of 1.64 nm and (b) 1.71 nm.

the tubule axis as that of each individual tubule. In these two cases, the bundle was aligned in such a way that the incident electron beam was oriented along the [100] direction of the hexagonal packing. Using the graphitic reflection (100) ($d_{100} = 0.2132$ nm) as a standard scale to calibrate the camera length, the super reflections in Fig. 4a give a hexagonal packing of lattice constant $A = 1.64$ nm and Fig. 4b gives $A = 1.71$ nm.

It should be pointed out here that these two values are different from previous results measured using X-ray diffraction [5] and high-resolution electron microscopy [9], which gave $A = 1.70$ nm [5] and $A = 1.59$ nm [9], respectively. These new values should reflect the fact that under the current synthesis conditions, carbon nanotubes of a variety of diameters and helicities were formed.

The information on the helicity distribution is important in understanding the growth morphology of nanotube bundles. When nanotubes grow together to form bundles, the helicity difference between neighboring tubules should have strong influence on the growing pattern. For example, if all tubules have a single helicity, parallel alignment of these tubules may be preferred, as discussed for the special case where all individual nanotubes were proposed to have the armchair structure [5]. However, when neighboring nanotubes have different helicities to form bundles, twisting could occur as a result of minimizing the formation energy. This in turn would present a new phenomenon of self-assembling of single-walled carbon nanotubes [10].

4. Conclusions

Most carbon nanotubes in raft-like bundles, produced by laser evaporation, have a quite uniform distribution of helicities among the constituting tubules, ranging from the zigzag structure of 0° helicity to the armchair structure of 30° helicity. As a rare encounter, a bundle of nanotubes of single helicity corresponding to the armchair structure has been identified for the first time in experiment using electron nanodiffraction. Carbon nanotubes of various size forming bundles were observed, for example, two different hexagonal lattice constants of 1.64 nm and 1.71 nm were determined from the respective electron nanodiffraction patterns.

Acknowledgements

This research is partially supported by NEDO International Joint Research Grant and Special Coordination Funds of the Science and Technology Agency of the Japanese Government.

References

[1] S. Iijima, Nature., 354 (1991) 56.
[2] S. Iijima and T. Ichihashi, Nature., 363 (1993) 603.
[3] N. Hamada, S. Sawada and A. Oshiyama, Phys. Rev. Lett., 68 (1992) 1579.
[4] O. Zhou, R.M. Fleming, D.W. Murphy, C.H. Chen, R.C. Haddon, A.P. Ramirez and S.H. Glarum, Science., 263 (1994) 1744.
[5] A. Thess, R. Lee, P. Nikolaev, H. Dai, P. Petit, J. Robert, C. Xu, Y.H. Lee, S.G. Kim, A.G. Rinzler, D.T. Colbert, G.E. Scuseria, D. Tomanek, J.E. Fisher and R.E. Smalley, Science., 273 (1996) 483.
[6] L.C. Qin, J. Mater. Res., 9 (1994) 2450.
[7] L.C. Qin, T. Ichihashi and S. Iijima, Ultramicroscopy (1996) in press.
[8] T. Guo, P. Nikolaev, A. Thess, D.T. Colbert and R.E. Smalley, Chem. Phys. Lett., 243 (1995) 149.
[9] L.C. Qin and S. Iijima, submitted to Chem. Phys. Lett.
[10] L.C. Qin and S. Iijima, to be published.